Title: Region-specific microRNA alterations in marmosets carrying SLC6A4 polymorphisms are associated to anxiety-like behavior.

Authors: Natalia Popa[1] PhD, Angela C. Roberts[2] PhD, Andrea M. Santangelo [2, ‡] PhD, and Eduardo Gascon [1,‡], MD, PhD.

[1] Aix Marseille Univ, CNRS, INT, Inst Neurosci Timone, Marseille, France

[2] Department of Physiology, Development and Neuroscience, University of Cambridge, Cambridge, United Kingdom

[3] Department of Physiology, Development and Neuroscience, Harvard University,

‡ Co-senior authors

*Corresponding author: Eduardo Gascon, Institut de Neurosciences de la Timone, Aix-Marseille Université; CNRS UMR7289; 27, Boulevard Jean Moulin, 13005 Marseille (France); E-mail: eduardo.gascon-gonzalo@univ-amu.fr

Keywords: anxiety, marmoset, microRNA, ventro-medial prefrontal cortex, DCC

Running title: Marmoset SLC6A4 polymorphisms, anxiety and region-specific miRNAs

SUMMARY

Human studies have consistently reported that stress-related disorders such as depression and anxiety impinge on the activity of emotion regulation networks, namely in the ventromedial prefrontal cortex (vmPFC). However, molecular heterogeneity, including microRNAs, within the vmPFC and how these differences affect emotion regulation and behavior have not been elucidated. Marmosets have emerged as a powerful model in translational neuroscience to investigate molecular underpinnings of complex behaviors. Here, we took advantage of naturally occurring genetic polymorphisms in marmoset *SLC6A4* gene that have been linked to anxiety-like behaviors in response to an ambiguous threat. Using FACS-sorted cells from different brain regions, we showed that marmosets bearing different *SLC6A4* variants exhibit distinct miRNAs signatures specifically in vmPFC area 32 neurons, but not in the closely related vmPFC area 25. We also identified DCC, a gene previously involved in anxiety and depression, as a downstream target of miRNAs deregulated in vmPFC area 32. Finally, we found that levels of DCC and miRNAs in area 32 were highly correlated to an anxiety score in a test of uncertain threat. To the best of our knowledge, this is the first report in primates providing experimental links between molecular alterations at specific vmPFC areas and complex behavioral responses in the context of genetic variants relevant to human psychopathology.

INTRODUCTION

Anxiety is a core symptom of multiple psychiatric disorders including depression and schizophrenia. A central goal in translational neuroscience is to better understand how aberrant brain function linked to such diseases arises from disruptions at the molecular level. It is widely accepted that anxiety stems from the evaluation of cost/benefits and/or the subsequent decision-making process (Corr et al., 2021; Millan, 2003; Oathes et al., 2015), functions that are highly dependent upon the prefrontal cortex (PFC). In particular, neuroimaging studies in humans have linked ventro-medial PFC (vmPFC) activity in cost-benefit decisions (Talmi et al., 2009; Tom et al., 2007) and in emotional responses under conflict situations (Egner et al., 2008; Hiser and Koenigs, 2018). Similarly, whilst decision variables appear widely represented across the frontal cortex of macaque monkeys (Kennerley et al., 2009; Mehta et al., 2019), neurons in the vmPFC have been specifically identified to encode the gain or cost associated with expected outcomes (Haroush and Williams, 2015; Hayden and Platt, 2010; Kennerley et al., 2009) as well as their emotional valence (Amemori and Graybiel, 2012; Amemori et al., 2015). Not surprisingly then, altered processing and deficiencies in vmPFC circuitry have been implicated in the enhanced negative emotion typical of anxiety and affective disorders (Hiser and Koenigs, 2018; Via et al., 2018). Activity in the vmPFC has also been shown not only to predict treatment efficacy but its normalization parallels remission (Kennedy et al., 2007; Fox et al., 2012) . It is important to recognize that the vmPFC encompasses distinct regions with marked, cellular composition, connectivity patterns and function (Hiser and Koenigs, 2018; Roberts and Clarke, 2019; Myers-Schulz and Koenigs, 2012; Stawicka et al., 2020; Wallis et al., 2019; Zeredo et al., 2019).

Of particular relevance to the vmPFC's involvement in the etiology and treatment of anxiety are its particularly high levels of the serotonin transporter, compared to the rest of the PFC (Way et al., 2007). Selective serotonin reuptake inhibitors that target the transporter are the first line treatment for anxiety and depression (Goodman, 2004) and genetic variants in the *SLC6A4* gene (encoding the serotonin transporter) (Lesch et al., 1996) or HTR1A (Lemonde et al., 2003; Strobel et al., 2003) are linked to a higher risk of anxiety and depression. Thus, understanding the cellular mechanisms by which serotonin regulates vmPFC function will help in the quest for more rational therapeutic targets in anxiety treatment. MicroRNAs (miRNAs) are attractive candidates as they have been shown to modulate such regulatory neurotransmitters and signaling cascades and to be de-regulated in patients with affective disorders (for review see (Allen and Dwivedi, 2020; Lopez et al., 2018). They are a class of short (20-25 nt) non-coding RNAs and one of the best-studied posttranscriptional modifiers of gene expression (Huntzinger and Izaurralde, 2011; Izaurralde, 2015). miRNAs repress expression of messenger RNAs (mRNAs) containing complementary sequences and have been involved in multiple pathological processes, including psychiatric diseases (Geaghan and Cairns, 2015; Yoshino and Dwivedi, 2020). In particular, the investigation of miRNAs in psychiatric disorders has gained momentum as accumulating evidences indicate that miRNAs could be potentially used as biomarkers and/or therapies (Belzeaux et al., 2017; Roy et al., 2020).

The common marmoset, *Callithrix jacchus*, has emerged as a reference model in modern neuroscience. Compared to rodents, marmosets are closer to humans, not only in their behavioral repertoire and brain organization, including vmPFC, but also in molecular terms (Finkenwirth et al., 2015; Miller et al., 2016). Recent studies in this

species have thus shown that *SLC6A4* polymorphisms affect the regulation of behaviors elicited by threat in the human intruder paradigm, the response to antidepressants and the neurochemical balance in brain areas implicated in emotional processing (Quah et al., 2020a; Quah et al., 2020b; Santangelo et al., 2016; Santangelo et al., 2019). In addition, recent studies have begun to reveal distinct functional units within the vmPFC (Alexander et al., 2019; Alexander et al., 2020). Here, we used marmosets carrying distinct *SLC6A4* haplotypes as the experimental model to dissect out molecular (namely in miRNAs) alterations linked to trait-like anxiety, within distinct regions of vmPFC. We found that *SLC6A4* variants result in miRNA alterations in a remarkably region-specific manner. We also identified DCC, a gene previously implicated in affective disorders, as a downstream target of the deregulated miRNA networks. Since such changes are highly correlated to behavioral responses, our results underscore the intimate link between molecular differences among vmPFC areas and complex behavioral outcomes.

RESULTS

microRNA profiling in the marmoset cortex discriminates between NeuN$^+$ and NeuN$^-$ cells across cortical areas

In order to investigate whether miRNAs signatures could be linked to behavioral responses, we first validated an experimental approach previously applied to human samples (Lutz et al., 2017) (Fig. 1a). Brains from genotyped and behaviorally phenotyped marmosets were sliced and punches from selected brain regions were harvested. After nuclear isolation, samples were FACS sorted into NeuN$^+$ and NeuN$^-$ cells (Suppl. Fig. 1a) and RNA extracted from each fraction. As expected, NeuN$^+$ cells are enriched in neuron-specific markers (Grm7, Gabra1, Camk2) and deprived almost entirely of glial-associated genes (astrocyte, oligodendrocytes and microglia markers, Fig. 1b and Suppl. Fig. 1b). In contrast, NeuN$^-$ cells express strong levels of astrocytes (Gfap, Aldh1l1 or Slc1a3), oligodendrocytes (Klk6, Plp1, Cnskr3) and microglial genes (Aif1) (Fig. 1B and Suppl. Fig. 1b). We also observe a low expression of neuronal genes in this fraction as it is known that a subset of neurons of the primate cortex are NeuN$^-$ (Lutz et al., 2017). Similar profiles were obtained in samples from different cortical regions (area 17, 25 and 32) indicating that FACS sorting is a reliable method to enrich neurons from different marmoset cortical areas for transcriptomic analysis.

Although miRNA expression in different brain cell types remains largely unexplored, we hypothesize that, given the differences in cell composition, miRNAs signatures present in NeuN$^+$ and NeuN$^-$ populations should be dramatically distinct. Using miRNA quantitative PCR, we profiled 754 miRNAs in our samples and found that almost 100 miRNAs were consistently expressed in both subpopulations. Using these miRNAs,

we performed a principal component analysis (PCA) in $NeuN^+$ and $NeuN^-$ nuclei coming from 6 different marmosets. As shown in Fig. 1c, $NeuN^+$ and $NeuN^-$ samples formed separated clustered across the PC1 axis confirming that, even considering only those miRNAs whose expression is shared, miRNAs profiles readily distinguish both fractions.

Recent work (Krienen et al., 2020) revealed important regional differences in gene expression across the marmoset cortex. We next investigated whether, similarly, miRNA profiling might be sensitive enough and detect such regional variations. For that purpose, we examined 3 cortical areas; on one hand, we profiled the primary visual cortex (corresponding to Brodmann area 17) as an example of sensory region endowed with specific cytoarchitectonic and functional features (e.g. expanded layer IV, strong myelination, major inputs from the thalamus). On the other hand, we considered two high-order association areas within the vmPFC (Brodmann area 25 and 32) whose activity has been shown to be consistently deregulated in affective disorders (Egner et al., 2008; Etkin et al., 2006). PCA on miRNA levels (154 miRNAs that are consistently detected in all $NeuN^+$ samples) from these different areas enabled reconstruction of such regional pattern in $NeuN^+$ cells (Fig. 1d) but not in $NeuN^-$ cells (Suppl. Fig. 1c). Samples from the visual cortex clustered together on one side of the PC1 axis indicating a clear segregation between sensory and association areas in terms of miRNAs signature. In contrast, the two regions of the PFC appeared intermingled. Accordingly, a number of miRNAs (Suppl. Fig. 1d) are differentially expressed in the visual cortex. Again, such regional pattern cannot be observed in the $NeuN^-$ fraction (Suppl. Fig. 1c) suggesting that anatomo-molecular differences largely

arise from neurons. Together, these findings support the notion that miRNAs profiling is a powerful method to uncover molecular differences in the brain.

microRNA profiling uncovers region-specific molecular differences in marmosets bearing different SLC6A4 variants/haplotypes

Genetic polymorphisms in the marmoset *SLC6A4* promoter region have been linked to high trait anxiety (Santangelo et al., 2016). Since primate vmPFC has been widely involved in emotional processing (Roberts and Clarke, 2019), we sought to determine whether miRNA profiling could unveil molecular differences in marmosets bearing the two most frequent *SLC6A4* haplotypes (AC/C/G versus CT/T/C) described previously [34]. For that purpose, we analyzed miRNAs contents in 3 marmosets for each variant. As depicted in Fig. 2a, PCA on $NeuN^+$ neurons showed two independent clusters in area 32 corresponding to each genotype suggesting that this region might be specifically affected by *SLC6A4* polymorphisms. No such pattern was observed either in the primary visual cortex or in area 25 arguing against a broad cortical effect of the polymorphism. In order to confirm this genetic effect, we carried out a 2-way ANOVA on the miRNA levels in each region. We found that area 32 exhibited a significant effect of genotype on the miRNA expression ($F(1, 4)=17.06$; $p=0.0145$) whereas this was not observed in areas 17 ($F(1, 4)= 2.419$; $p=0.1949$) and 25 ($F(1, 4)=0.1311$; $p=0.1311$).

To determine which miRNAs are significantly and specifically deregulated in area 32 (differentially expressed miRNAs, DEmiRs), we took into account our results from the PCA and considered a list of 25 miRNAs that contributed the most to the first two PCs

(Table 1). miRNAs that exhibited differential expression in area 32 but not in BA17 and 25 are shown in Fig. 2b.

To confirm the specificity of this observations, we also analyzed neuronal miRNAs the expression of which is associated with visual cortex. Although a number of miRNAs (miR-195, miR-221, miR-222 and miR-497) were found to be differentially expressed in the visual cortex compared to area 25 and 32 (Suppl. Fig. 2), none of the BA17 DEmiRs showed any difference across the genotypes suggesting that there exist miRNAs whose expression is altered in precise regions in a genotype-dependent manner. Overall, our observations confirm that miRNAs could reliably uncover molecular differences in the marmoset cortex and indicate *SLC6A4* polymorphisms selectively alter miRNA signatures in area 32.

Genotype-specific changes of DCC expression in area 32

miRNAs regulate gene expression post-transcriptionally. We reasoned that miRNAs alterations in area 32 would result in significant changes in downstream target transcripts. To identify those targets and thus further validate our miRNAs signatures, we carried out a network analysis of the area 32 deregulated miRNAs using miRNet (Chang et al., 2020) (Fig 3a). We restricted our analysis using two criteria: i) target genes bearing binding sequences for, at least, three of the miRNAs differentially expressed in area 32 across *SLC6A4* variants; and ii) a coefficient correcting for miRNA abundance. Thus, we profiled the expression of 20 target genes as well as 15 control transcripts in area 25 and 32. None of the target mRNAs show significant changes in area 25 (Suppl. Fig. 3). In contrast, in area 32, DCC, was found to be differentially expressed across *SLC6A4* genotypes. DCC is the netrin receptor and recent work has

associated their expression in the prefrontal cortex to depression and anxiety (Li et al., 2020; Manitt et al., 2013; Torres-Berrío et al., 2017; Torres-Berrío et al., 2020a). DCC transcript contains putative sequences for miR-9-5p, let7-5p and miR-190. Levels of DCC were reduced in CT/T/C marmosets and inversely correlated to the levels of BA32-deregulated miRNAs (higher in CT/T/C animals, Fig. 2b). Despite the number of miRNA sequences present in DCC mRNA, the observed downregulation was moderate, in agreement with the contention that miRNAs fine-tune gene expression (Torres-Berrío et al., 2020b; Torres-Berrío et al., 2020c). Finally, we observed no reduction of DCC in area 25 (Suppl. Fig. 3) and no alteration of the reference transcripts in either BA25 or 32. Overall, our findings argue again for the anatomical specificity of molecular alterations associated to *SLC6A4* polymorphisms.

Molecular alterations in area 32 correlate with behavioral response to uncertain threat

It has been previously shown that *SLC6A4* polymorphisms strongly influence anxiety-like behavior in response to uncertainty in the human intruder test (HI-test), but do not alter evoked fear-like behavior in the more certain context of the snake test (ST) (Quah et al., 2020a; Santangelo et al., 2016). Using exploratory factor analysis (EFA), a recent study demonstrated that a single factor in the EFA explained behavior on the HI test whereas two factors were necessary to describe behaviors elicited on the ST (Quah et al., 2020b).

We reasoned that, if relevant, the molecular alterations identified in area 32 might correlate with behavioral responses in the HI-test but not the snake test. We therefore performed a correlation analysis on the levels of miRNAs deregulated with the EFA score for HI-test. We observed a significant negative correlation for four miRNAs in

area 32 (Fig. 4a), showing a R^2 coefficient ranging from 0.45 to 0.94; miR-525-3p showed the strongest association with an R^2=0.94 (p=.0013), followed by miR-125b-5p (R^2=0.78; p=.0197), let-7d-5p (R^2=0.69; p=.0393) and miR-125a-5p (R^2=0.68; p=.0407). Remarkably, DCC contents also show a significant but inverted correlation to the behavioral score (R^2=.899; p=.0039). In contrast, levels of the same miRNAs and DCC in area 25 exhibited no correlation with the HI test EFA (Fig. 4) arguing for the specificity of our findings. Moreover, the two behavioral scores in the ST were also not correlated with any of these miRNAs (Suppl. Fig. 4) supporting the notion that the molecular alterations we found in area 32 are connected to the differential behavioral response to uncertain threat in marmosets bearing the different *SLC6A4* variants.

DISCUSSION

Using a novel approach to investigate miRNA signatures, we show here specific molecular alterations underlying the anxiety-related *SLC6A4* polymorphisms within distinct regions of the primate vmPFC. Focusing on miRNAs in areas 32 and 25, with primary visual area 17 acting as a control region, we show that: i) miRNAs repertoire is dramatically different across cell types and cortical regions; ii) *SLC6A4* polymorphisms impinge selectively on miRNA signature in area 32; and iii) miRNA as well as target gene levels specifically in area 32 correlate with anxiety-like behavior in response to an uncertain threat. Although descriptive and based on a limited number of samples, our results support the notion that genetic differences might critically alter molecular pathways within specific cortical regions and that these changes perturb the behavioral repertoire.

The paucity of appropriate experimental models has precluded anatomical and molecular investigation of vmPFC in anxiety-like behaviors. Marmosets have emerged as an attractive model in translational neuroscience (Miller et al., 2016). Previous work has clearly demonstrated that naturally occurring polymorphisms in the Slc6a4 promoter region are linked to anxious-like behaviors (Santangelo et al., 2016; Santangelo et al., 2019). In addition, marmoset vmPFC parcellation appears to be markedly similar to that found in humans (Roberts and Clarke, 2019; Schaeffer et al., 2020) . Although both peri- and subgenual cortex have been consistently implicated in threat processing and stress-related disorders, it has been difficult to establish their functional differences. A recent study (Ironside et al., 2020) used a common approach-avoidance task in macaques and humans (both healthy controls and depressed patients) to compare

fMRI data. Interestingly, this work highlighted a shared primate network for aversive behavior. This circuit involved the perigenual but not subgenual cingulate cortex and was deregulated in patients. In the marmoset, previous work has clearly demonstrated the functional differences between marmoset area 25 and area 32 in threat reactivity, not only in the extinction of Pavlovian conditioned threat responses but also in approach-avoidance decision making (Wallis et al., 2019). In addition, overactivation of area 25 specifically evokes anxiety-like behavior in response to uncertainty evoked in the HI threat test (Alexander et al., 2020). However, the involvement of area 32 has not been addressed yet in this paradigm. In light of our findings and the mentioned work, future experiments using opto/chemogenetics should be carried out in the marmoset to precisely delineate the contribution of each area in the HI test.

Our study provides evidence supporting that miRNA alterations in area 32 affect the expression of target genes. Thus, animals bearing the CT/T/C variant show an increase of miRNAs regulating DCC, whose levels are accordingly downregulated in area 32 but not in area 25. It is worth highlighting that, rather than switching on and off gene expression, changes in brain miRNAs lead to modest reductions of target mRNAs (Rajman and Schratt, 2017; Schratt, 2009). Nonetheless, miRNA-dependent fine-tuning of specific targets has been consistently involved in the physiopathology of stress-related disorders (Fiori et al., 2020; Lopez et al., 2017; Torres-Berrío et al., 2017). DCC is the cognate receptor for netrin, a guidance cue involved in axon navigation during development (Tessier-Lavigne and Goodman, 1996). Remarkably, mutations in human *DCC* have been linked to human pathology (Srour et al., 2010), including stress-related disorders (Li et al., 2020; Manitt et al., 2013; Torres-Berrío et al., 2017). Recent data suggest that DCC expression in the prefrontal cortex is particularly high during the

adolescence and that DCC levels might contribute to vulnerability to stress-related disorders in mice (Torres-Berrío et al., 2020b; Torres-Berrío et al., 2020c). In agreement with these observations, we show a clear correlation between DCC contents in area 32 and anxious-like behaviors (Fig. 4). Since this is not the case in area 25, our findings indicate that DCC function might be essential for proper function of specific vmPFC circuits. Future experiments should examine DCC expression among vmPFC regions in detail.

Recent work has demonstrated that miR-218 tightly regulates DCC expression in the mouse brain (Torres-Berrío et al., 2020b; Torres-Berrío et al., 2020c). Importantly, miRNA-mediated silencing of DCC has been shown to be a key event in susceptibility to stress-related disorders (Torres-Berrío et al., 2017). In our marmosets, miR-218 is clearly more abundant in the prefrontal cortex (both in area 25 and 32) than in the visual cortex (Suppl. Fig. 5). However, we could not reveal any difference in miR-218 levels across genotypes (Suppl. Fig. 5). Instead, our work provide evidence that alternative miRNAs might might contribute to fine-tune DCC contents in a region-dependent manner. In this line, human studies have already implicated some of the miRNAs identified here such as miR-9-5p or let-7d-5p in psychiatric conditions (Camkurt et al., 2020; He et al., 2021; Maffioletti et al., 2016). Moreover, work in rodents have provided initial experimental evidences confirming such links (Bahi and Dreyer, 2018; Ma et al., 2019; Zhang et al., 2020). Future work is definitely required to identify the cellular mechanisms by which Slc6a4 variants alters miRNAs and DCC levels in precise cortical areas.

From a molecular perspective, recent data using single-cell RNA sequencing have provided experimental evidences of the existence of unique neuronal types and primate-specific genetic programs (Hodge et al., 2019; Krienen et al., 2020). In the same line, the repertoire of non-coding RNAs (ncRNAs) has expanded across evolution and multiple studies support the notion that primate-restricted ncRNAs contribute to psychiatric conditions including depression (Issler et al., 2020; Lopez et al., 2014). Building on these findings, our results reveal a primate-specific miRNA, miR-525-3p, the levels of which are best correlated with uncertainty-evoked anxiety-like, as distinct from direct, threat-evoked, fear-like behavior. miR-525 is an evolutionary recent miRNA as shown by the exact sequence conservation between human, gorilla, and chimpanzee. A less conserved sequence is found in other old-world (orangutan, baboon and macaques) and new-world monkeys (marmosets and squirrel monkeys) but not in prosimians (mouse lemur) suggesting that a common miR-525 ancestor appeared about 40 million years ago (Suppl. Fig. 6). Our results highlight the importance of molecular investigations in the brains of primates that might uncover evolutionary recent molecular pathways of utmost interest for translational psychiatry.

Investigating the reactivity of marmosets to direct/immediate and more uncertain/ambiguous threat as revealed by responsivity to a rubber snake and an unknown human provides experimental settings in which to model different aspects of anxiety-like and fear-like behaviors which likely engage distinct neural networks and psychological processes. In humans, reactivity to immediate threat has been shown to engage dorsal cingulate and brainstem circuitry, whilst reactivity to more ambiguous, potentially distal threat has been shown to engage higher-order prefrontal brain regions (Mobbs et al., 2020). Our finding here that molecular differences between

individuals bearing specific *SLC6A4* variants are specifically associated with area 32 and are related to reactivity to uncertain, but not certain threat, is consistent with this. Given the known involvement of serotonin in brain development (Suri et al., 2015) future studies should determine the relationship of such variants within the developing brain, in particular, the process by which area 32 integrates into prefrontal executive networks. This is highly relevant to our understanding of the onset of psychiatric disorders since the majority begin during adolescence (Keshavan et al., 2014; Kessler et al., 2005), a period in which miRNAs changes might significantly contribute to brain vulnerability (Torres-Berrío et al., 2020b; Torres-Berrío et al., 2020c).

ACKNOWLEDGEMENTS

This work was supported by France National Agency (ANR18-CE37-0017), NRJ foundation, Celphedia and Fondation de France (00100077) to EG and a Wellcome Trust Investigator award (108089/Z/15/Z) to A.C.R.

AUTHOR CONTRIBUTIONS

ACR, AMS and EG conceived and designed the project. AMS performed the behavioral testing and sample preparation. NP performed miRNA and gene expression experiments. NP, AMS and EG analyzed the data. ACR provided contribution to the interpretation of data. AMS, ACR and EG wrote the manuscript. NP, ACR, AMS and EG discussed the results, reviewed and edited the final manuscript. We would like to thank Stephane Robert from the AMUTICYT facility for his precious support for the FACS sorting.

DECLARATION OF INTEREST

The authors report no biomedical financial interests or potential conflicts of interest.

FIGURE LEGENDS

Figure 1. Schematic representation of experimental protocol and validation steps.

a) Experimental protocol included the genotypic and phenotypic characterization of the marmosets. After sacrifice, brains were frozen and sliced without fixation. RNA was extracted from punches of different cortical regions. Samples were subsequently submitted to nuclear isolation, NeuN staining and FACS sorting.

b) Expression of neuronal (top panel), astrocytic (middle panel) and oligodendrocytic (bottom panels) markers in $NeuN^+$ and $NeuN^-$ fractions confirmed the efficiency of the FACS sorting strategy.

c) PCA analysis on the levels of 92 miRNAs expressed in both $NeuN^+$ and $NeuN^-$ nuclei demonstrated that miRNAs profiles clearly differentiate both fractions.

d) PCA analysis on miRNAs level in $NeuN^+$ fraction enabled regional discrimination. Samples from the visual cortex clearly clustered apart from those of the vmPFC which, in turn, are intermingled.

Figure 2. SLC6A4 polymorphisms (AC/C/G and CT/T/C) and miRNA signature in area 32.

a) PCA analysis on miRNAs level in $NeuN^+$ nuclei showed genotypic differences only in area 32.

b) miRNAs differentially expressed in area 32 in AC/C/G and CT/T/C marmosets (One way ANOVA followed by Bonferroni's test for multiple comparisons, * $p<.05$).

Figure 3. Expression of target mRNAs.

a) Network analysis using miRNAs deregulated in area 32.

b) Expression of target mRNAs identified by network analysis in area 32 and 25. Using as reference the AC/C/G genotype, we measured the abundance of 20 potential targets as well as 15 reference genes. Only Dcc was found to be differentially expressed in area 32 ($p=0.0483$, 2-way ANOVA followed by Tukey test for multiple comparisons, $p<0.05$)

Figure 4. Correlation between miRNA / Dcc levels in area 32 (left panels) or 25 (right panels) and behavioral response in the human intruder test.

Table 1. Statistical analysis of expression levels of top 25 miRNAs from PCA (One-way ANOVA adjusted for multiple comparison with Bonferroni's correction).

miRNA	**Area 25 (AC vs CT)** **Adjusted p value**	**Area 32 (AC vs CT)** **Adjusted p value**
let-7a-5p	>0.999	0.1181
let-7d-5p	>0.999	**0.0208**
miR-9-5p	0.9891	**0.0475**
miR-26a-5p	>0.999	0.4908
miR-100-5p	0.2004	0.1486
miR-124-3p	0.3564	0.1234
miR-125a-5p	>0.999	**0.0013**
miR-125b-5p	0.4031	**0.0196**
miR-129-1-3p	0.2080	0.6278
miR-133a-5p	>0.999	0.8187
miR-144-3p	>0.999	>0.999
miR-190a-5p	>0.999	**0.0032**
miR-195-5p	>0.999	0.6839
miR-200a-3p	>0.999	0.1737
miR-221-3p	>0.999	>0.999
miR-222-3p	>0.999	0.4192
miR-302b-3p	0.2303	0.5073
miR-320a	0.9693	>0.999
miR-376a-3p	0.5647	>0.999
miR-378a-3p	>0.999	0.0554

miR-495-3p	>0.999	>0.999
miR-497-5p	0.9585	0.6780
miR-525-3p	0.3089	**0.0019**
miR-628-3p	>0.999	>0.999
miR-645	0.4508	>0.999

REFERENCES

Alexander, L., Gaskin, P. L. R., Sawiak, S. J., Fryer, T. D., Hong, Y. T., Cockcroft, G. J., Clarke, H. F., and Roberts, A. C. (2019). Fractionating Blunted Reward Processing Characteristic of Anhedonia by Over-Activating Primate Subgenual Anterior Cingulate Cortex. Neuron *101*, 307-320.e6.

Alexander, L., Wood, C. M., Gaskin, P. L. R., Sawiak, S. J., Fryer, T. D., Hong, Y. T., McIver, L., Clarke, H. F., and Roberts, A. C. (2020). Over-activation of primate subgenual cingulate cortex enhances the cardiovascular, behavioral and neural responses to threat. Nat Commun *11*, 5386.

Allen, L., and Dwivedi, Y. (2020). MicroRNA mediators of early life stress vulnerability to depression and suicidal behavior. Mol Psychiatry *25*, 308-320.

Amemori, K., Amemori, S., and Graybiel, A. M. (2015). Motivation and affective judgments differentially recruit neurons in the primate dorsolateral prefrontal and anterior cingulate cortex. J Neurosci *35*, 1939-1953.

Amemori, K., and Graybiel, A. M. (2012). Localized microstimulation of primate pregenual cingulate cortex induces negative decision-making. Nat Neurosci *15*, 776-785.

Bahi, A., and Dreyer, J. L. (2018). Lentiviral-mediated let-7d microRNA overexpression induced anxiolytic- and anti-depressant-like behaviors and impaired dopamine D3 receptor expression. Eur Neuropsychopharmacol *28*, 1394-1404.

Barros, M., Boere, V., Huston, J. P., and Tomaz, C. (2000). Measuring fear and anxiety in the marmoset (Callithrix penicillata) with a novel predator confrontation model: effects of diazepam. Behav Brain Res *108*, 205-211.

Belzeaux, R., Lin, R., and Turecki, G. (2017). Potential Use of MicroRNA for Monitoring Therapeutic Response to Antidepressants. CNS Drugs *31*, 253-262.

Camkurt, M. A., Karababa, İ. F., Erdal, M. E., Kandemir, S. B., Fries, G. R., Bayazıt, H., Ay, M. E., Kandemir, H., Ay, Ö. I., Coşkun, S., Çiçek, E., and Selek, S. (2020). MicroRNA dysregulation in manic and euthymic patients with bipolar disorder. J Affect Disord *261*, 84-90.

Carey, G. J., Costall, B., Domeney, A. M., Jones, D. N., and Naylor, R. J. (1992). Behavioural effects of anxiogenic agents in the common marmoset. Pharmacol Biochem Behav *42*, 143-153.

Chang, L., Zhou, G., Soufan, O., and Xia, J. (2020). miRNet 2.0: network-based visual analytics for miRNA functional analysis and systems biology. Nucleic Acids Res *48*, W244-W251.

Corr, R., Pelletier-Baldelli, A., Glier, S., Bizzell, J., Campbell, A., and Belger, A. (2021). Neural mechanisms of acute stress and trait anxiety in adolescents. Neuroimage Clin *29*, 102543.

Egner, T., Etkin, A., Gale, S., and Hirsch, J. (2008). Dissociable neural systems resolve conflict from emotional versus nonemotional distracters. Cereb Cortex *18*, 1475-1484.

Etkin, A., Egner, T., Peraza, D. M., Kandel, E. R., and Hirsch, J. (2006). Resolving emotional conflict: a role for the rostral anterior cingulate cortex in modulating activity in the amygdala. Neuron *51*, 871-882.

Finkenwirth, C., van Schaik, C., Ziegler, T. E., and Burkart, J. M. (2015). Strongly bonded family members in common marmosets show synchronized fluctuations in oxytocin. Physiol Behav *151*, 246-251.

Fiori, L. M., Kos, A., Lin, R., Théroux, J. F., Lopez, J. P., Kühne, C., Eggert, C., Holzapfel, M., Huettl, R. E., Mechawar, N., Belzung, C., Ibrahim, E. C., Chen, A., and Turecki, G. (2020). miR-323a regulates ERBB4 and is involved in depression. Mol Psychiatry

Fox, M. D., Buckner, R. L., White, M. P., Greicius, M. D., and Pascual-Leone, A. (2012). Efficacy of transcranial magnetic stimulation targets for depression is related to intrinsic functional connectivity with the subgenual cingulate. Biol Psychiatry *72*, 595-603.

Geaghan, M., and Cairns, M. J. (2015). MicroRNA and Posttranscriptional Dysregulation in Psychiatry. Biol Psychiatry *78*, 231-239.

Goodman, W. K. (2004). Selecting pharmacotherapy for generalized anxiety disorder. J Clin Psychiatry *65 Suppl 13*, 8-13.

Haroush, K., and Williams, Z. M. (2015). Neuronal prediction of opponent's behavior during cooperative social interchange in primates. Cell *160*, 1233-1245.

Hayden, B. Y., and Platt, M. L. (2010). Neurons in anterior cingulate cortex multiplex information about reward and action. J Neurosci *30*, 3339-3346.

He, C., Bai, Y., Wang, Z., Fan, D., Wang, Q., Liu, X., Zhang, H., Zhang, H., Zhang, Z., Yao, H., and Xie, C. (2021). Identification of microRNA-9 linking the effects of childhood maltreatment on depression using amygdala connectivity. Neuroimage *224*, 117428.

Hiser, J., and Koenigs, M. (2018). The Multifaceted Role of the Ventromedial Prefrontal Cortex in Emotion, Decision Making, Social Cognition, and Psychopathology. Biol Psychiatry *83*, 638-647.

Hodge, R. D., Bakken, T. E., Miller, J. A., Smith, K. A., Barkan, E. R., Graybuck, L. T., Close, J. L., Long, B., Johansen, N., Penn, O., Yao, Z., Eggermont, J., Höllt, T., Levi, B. P., Shehata, S. I., Aevermann, B., Beller, A., Bertagnolli, D., Brouner, K., Casper, T., Cobbs, C., Dalley, R., Dee, N., Ding, S. L., Ellenbogen, R. G., Fong, O., Garren, E., Goldy, J., Gwinn, R. P., Hirschstein, D., Keene, C. D., Keshk, M., Ko, A. L., Lathia, K., Mahfouz, A., Maltzer, Z., McGraw, M., Nguyen, T. N., Nyhus, J., Ojemann, J. G., Oldre, A., Parry, S., Reynolds, S., Rimorin, C., Shapovalova, N. V., Somasundaram, S., Szafer, A., Thomsen, E. R., Tieu, M., Quon, G., Scheuermann, R. H., Yuste, R., Sunkin, S. M., Lelieveldt, B., Feng, D., Ng, L., Bernard, A., Hawrylycz, M., Phillips, J. W., Tasic, B., Zeng, H., Jones, A. R., Koch, C., and Lein, E. S. (2019). Conserved cell types with divergent features in human versus mouse cortex. Nature *573*, 61-68.

Huntzinger, E., and Izaurralde, E. (2011). Gene silencing by microRNAs: contributions of translational repression and mRNA decay. Nat Rev Genet *12*, 99-110.

Ironside, M., Amemori, K. I., McGrath, C. L., Pedersen, M. L., Kang, M. S., Amemori, S., Frank, M. J., Graybiel, A. M., and Pizzagalli, D. A. (2020). Approach-Avoidance Conflict in Major Depressive Disorder: Congruent Neural Findings in Humans and Nonhuman Primates. Biol Psychiatry *87*, 399-408.

Issler, O., van der Zee, Y. Y., Ramakrishnan, A., Wang, J., Tan, C., Loh, Y. E., Purushothaman, I., Walker, D. M., Lorsch, Z. S., Hamilton, P. J., Peña, C. J., Flaherty, E., Hartley, B. J., Torres-Berrío, A., Parise, E. M., Kronman, H., Duffy, J. E., Estill, M. S., Calipari, E. S., Labonté, B., Neve, R. L., Tamminga, C. A., Brennand, K. J., Dong, Y., Shen, L., and Nestler, E. J. (2020). Sex-Specific Role for the Long Non-coding RNA LINC00473 in Depression. Neuron *106*, 912-926.e5.

Izaurralde, E. (2015). GENE REGULATION. Breakers and blockers—miRNAs at work. Science *349*, 380-382.

Kennedy, S. H., Konarski, J. Z., Segal, Z. V., Lau, M. A., Bieling, P. J., McIntyre, R. S., and Mayberg, H. S. (2007). Differences in brain glucose metabolism between responders to CBT and venlafaxine in a 16-week randomized controlled trial. Am J Psychiatry *164*, 778-788.

Kennerley, S. W., Dahmubed, A. F., Lara, A. H., and Wallis, J. D. (2009). Neurons in the frontal lobe encode the value of multiple decision variables. J Cogn Neurosci *21*, 1162-1178.

Keshavan, M. S., Giedd, J., Lau, J. Y., Lewis, D. A., and Paus, T. (2014). Changes in the adolescent brain and the pathophysiology of psychotic disorders. Lancet Psychiatry *1*, 549-558.

Kessler, R. C., Berglund, P., Demler, O., Jin, R., Merikangas, K. R., and Walters, E. E. (2005). Lifetime prevalence and age-of-onset distributions of DSM-IV disorders in the National Comorbidity Survey Replication. Arch Gen Psychiatry *62*, 593-602.

Krienen, F. M., Goldman, M., Zhang, Q., C H Del Rosario, R., Florio, M., Machold, R., Saunders, A., Levandowski, K., Zaniewski, H., Schuman, B., Wu, C., Lutservitz, A., Mullally, C. D., Reed, N., Bien, E., Bortolin, L., Fernandez-Otero, M., Lin, J. D., Wysoker, A., Nemesh, J., Kulp, D., Burns, M., Tkachev, V., Smith, R., Walsh, C. A., Dimidschstein, J., Rudy, B., S Kean, L., Berretta, S., Fishell, G., Feng, G., and McCarroll, S. A. (2020). Innovations present in the primate interneuron repertoire. Nature *586*, 262-269.

Lemonde, S., Turecki, G., Bakish, D., Du, L., Hrdina, P. D., Bown, C. D., Sequeira, A., Kushwaha, N., Morris, S. J., Basak, A., Ou, X. M., and Albert, P. R. (2003). Impaired repression at a 5-hydroxytryptamine 1A receptor gene polymorphism associated with major depression and suicide. J Neurosci *23*, 8788-8799.

Lesch, K. P., Bengel, D., Heils, A., Sabol, S. Z., Greenberg, B. D., Petri, S., Benjamin, J., Müller, C. R., Hamer, D. H., and Murphy, D. L. (1996). Association of anxiety-related traits with a polymorphism in the serotonin transporter gene regulatory region. Science *274*, 1527-1531.

Li, H. J., Qu, N., Hui, L., Cai, X., Zhang, C. Y., Zhong, B. L., Zhang, S. F., Chen, J., Xia, B., Wang, L., Jia, Q. F., Li, W., Chang, H., Xiao, X., Li, M., and Li, Y. (2020). Further

confirmation of netrin 1 receptor (DCC) as a depression risk gene via integrations of multi-omics data. Transl Psychiatry *10*, 98.

Lopez, J. P., Fiori, L. M., Cruceanu, C., Lin, R., Labonte, B., Cates, H. M., Heller, E. A., Vialou, V., Ku, S. M., Gerald, C., Han, M. H., Foster, J., Frey, B. N., Soares, C. N., Müller, D. J., Farzan, F., Leri, F., MacQueen, G. M., Feilotter, H., Tyryshkin, K., Evans, K. R., Giacobbe, P., Blier, P., Lam, R. W., Milev, R., Parikh, S. V., Rotzinger, S., Strother, S. C., Lewis, C. M., Aitchison, K. J., Wittenberg, G. M., Mechawar, N., Nestler, E. J., Uher, R., Kennedy, S. H., and Turecki, G. (2017). MicroRNAs 146a/b-5 and 425-3p and 24-3p are markers of antidepressant response and regulate MAPK/Wnt-system genes. Nat Commun *8*, 15497.

Lopez, J. P., Kos, A., and Turecki, G. (2018). Major depression and its treatment: microRNAs as peripheral biomarkers of diagnosis and treatment response. Curr Opin Psychiatry *31*, 7-16.

Lopez, J. P., Lim, R., Cruceanu, C., Crapper, L., Fasano, C., Labonte, B., Maussion, G., Yang, J. P., Yerko, V., Vigneault, E., El Mestikawy, S., Mechawar, N., Pavlidis, P., and Turecki, G. (2014). miR-1202 is a primate-specific and brain-enriched microRNA involved in major depression and antidepressant treatment. Nat Med *20*, 764-768.

Lutz, P. E., Tanti, A., Gasecka, A., Barnett-Burns, S., Kim, J. J., Zhou, Y., Chen, G. G., Wakid, M., Shaw, M., Almeida, D., Chay, M. A., Yang, J., Larivière, V., M'Boutchou, M. N., van Kempen, L. C., Yerko, V., Prud'homme, J., Davoli, M. A., Vaillancourt, K., Théroux, J. F., Bramoullé, A., Zhang, T. Y., Meaney, M. J., Ernst, C., Côté, D., Mechawar, N., and Turecki, G. (2017). Association of a History of Child Abuse With Impaired Myelination in the Anterior Cingulate Cortex: Convergent Epigenetic, Transcriptional, and Morphological Evidence. Am J Psychiatry *174*, 1185-1194.

Ma, Z. Y., Chen, F., Xiao, P., Zhang, X. M., and Gao, X. X. (2019). Silence of MiR-9 protects depression mice through Notch signaling pathway. Eur Rev Med Pharmacol Sci *23*, 4961-4970.

Maffioletti, E., Cattaneo, A., Rosso, G., Maina, G., Maj, C., Gennarelli, M., Tardito, D., and Bocchio-Chiavetto, L. (2016). Peripheral whole blood microRNA alterations in major depression and bipolar disorder. J Affect Disord *200*, 250-258.

Manitt, C., Eng, C., Pokinko, M., Ryan, R. T., Torres-Berrío, A., Lopez, J. P., Yogendran, S. V., Daubaras, M. J., Grant, A., Schmidt, E. R., Tronche, F., Krimpenfort, P., Cooper, H. M., Pasterkamp, R. J., Kolb, B., Turecki, G., Wong, T. P., Nestler, E. J., Giros, B., and Flores, C. (2013). dcc orchestrates the development of the prefrontal cortex during adolescence and is altered in psychiatric patients. Transl Psychiatry *3*, e338.

Mehta, P. S., Tu, J. C., LoConte, G. A., Pesce, M. C., and Hayden, B. Y. (2019). Ventromedial Prefrontal Cortex Tracks Multiple Environmental Variables during Search. J Neurosci *39*, 5336-5350.

Millan, M. J. (2003). The neurobiology and control of anxious states. Prog Neurobiol *70*, 83-244.

Miller, C. T., Freiwald, W. A., Leopold, D. A., Mitchell, J. F., Silva, A. C., and Wang, X. (2016). Marmosets: A Neuroscientific Model of Human Social Behavior. Neuron *90*, 219-233.

Mobbs, D., Headley, D. B., Ding, W., and Dayan, P. (2020). Space, Time, and Fear: Survival Computations along Defensive Circuits. Trends Cogn Sci *24*, 228-241.

Myers-Schulz, B., and Koenigs, M. (2012). Functional anatomy of ventromedial prefrontal cortex: implications for mood and anxiety disorders. Mol Psychiatry *17*, 132-141.

Oathes, D. J., Patenaude, B., Schatzberg, A. F., and Etkin, A. (2015). Neurobiological signatures of anxiety and depression in resting-state functional magnetic resonance imaging. Biol Psychiatry *77*, 385-393.

Quah, S. K. L., Cockcroft, G. J., McIver, L., Santangelo, A. M., and Roberts, A. C. (2020a). Avoidant Coping Style to High Imminence Threat Is Linked to Higher Anxiety-Like Behavior. Front Behav Neurosci *14*, 34.

Quah, S. K. L., McIver, L., Roberts, A. C., and Santangelo, A. M. (2020b). Trait Anxiety Mediated by Amygdala Serotonin Transporter in the Common Marmoset. J Neurosci *40*, 4739-4749.

Rajman, M., and Schratt, G. (2017). MicroRNAs in neural development: from master regulators to fine-tuners. Development *144*, 2310-2322.

Roberts, A. C., and Clarke, H. F. (2019). Why we need nonhuman primates to study the role of ventromedial prefrontal cortex in the regulation of threat- and reward-elicited responses. Proc Natl Acad Sci U S A

Roy, B., Yoshino, Y., Allen, L., Prall, K., Schell, G., and Dwivedi, Y. (2020). Exploiting Circulating MicroRNAs as Biomarkers in Psychiatric Disorders. Mol Diagn Ther *24*, 279-298.

Santangelo, A. M., Ito, M., Shiba, Y., Clarke, H. F., Schut, E. H., Cockcroft, G., Ferguson-Smith, A. C., and Roberts, A. C. (2016). Novel Primate Model of Serotonin Transporter Genetic Polymorphisms Associated with Gene Expression, Anxiety and Sensitivity to Antidepressants. Neuropsychopharmacology *41*, 2366-2376.

Santangelo, A. M., Sawiak, S. J., Fryer, T., Hong, Y., Shiba, Y., Clarke, H. F., Riss, P. J., Ferrari, V., Tait, R., Suckling, J., Aigbirhio, F. I., and Roberts, A. C. (2019). Insula serotonin 2A receptor binding and gene expression contribute to serotonin transporter polymorphism anxious phenotype in primates. Proc Natl Acad Sci U S A *116*, 14761-14768.

Schaeffer, D. J., Hori, Y., Gilbert, K. M., Gati, J. S., Menon, R. S., and Everling, S. (2020). Divergence of rodent and primate medial frontal cortex functional connectivity. Proc Natl Acad Sci U S A *117*, 21681-21689.

Schratt, G. (2009). Fine-tuning neural gene expression with microRNAs. Curr Opin Neurobiol *19*, 213-219.

Shiba, Y., Santangelo, A. M., Braesicke, K., Agustín-Pavón, C., Cockcroft, G., Haggard, M., and Roberts, A. C. (2014). Individual differences in behavioral and cardiovascular reactivity to emotive stimuli and their relationship to cognitive flexibility in a primate model of trait anxiety. Front Behav Neurosci *8*, 137.

Srour, M., Rivière, J. B., Pham, J. M., Dubé, M. P., Girard, S., Morin, S., Dion, P. A., Asselin, G., Rochefort, D., Hince, P., Diab, S., Sharafaddinzadeh, N., Chouinard, S., Théoret, H., Charron, F., and Rouleau, G. A. (2010). Mutations in DCC cause congenital mirror movements. Science *328*, 592.

Stawicka, Z. M., Massoudi, R., Horst, N. K., Koda, K., Gaskin, P. L. R., Alexander, L., Santangelo, A. M., McIver, L., Cockcroft, G. J., Wood, C. M., and Roberts, A. C. (2020).

Ventromedial prefrontal area 14 provides opposing regulation of threat and reward-elicited responses in the common marmoset. Proc Natl Acad Sci U S A *117*, 25116-25127.

Strobel, A., Gutknecht, L., Rothe, C., Reif, A., Mössner, R., Zeng, Y., Brocke, B., and Lesch, K. P. (2003). Allelic variation in 5-HT1A receptor expression is associated with anxiety- and depression-related personality traits. J Neural Transm (Vienna) *110*, 1445-1453.

Suri, D., Teixeira, C. M., Cagliostro, M. K., Mahadevia, D., and Ansorge, M. S. (2015). Monoamine-sensitive developmental periods impacting adult emotional and cognitive behaviors. Neuropsychopharmacology *40*, 88-112.

Talmi, D., Dayan, P., Kiebel, S. J., Frith, C. D., and Dolan, R. J. (2009). How humans integrate the prospects of pain and reward during choice. J Neurosci *29*, 14617-14626.

Tessier-Lavigne, M., and Goodman, C. S. (1996). The molecular biology of axon guidance. Science *274*, 1123-1133.

Tom, S. M., Fox, C. R., Trepel, C., and Poldrack, R. A. (2007). The neural basis of loss aversion in decision-making under risk. Science *315*, 515-518.

Torres-Berrío, A., Hernandez, G., Nestler, E. J., and Flores, C. (2020a). The Netrin-1/DCC Guidance Cue Pathway as a Molecular Target in Depression: Translational Evidence. Biol Psychiatry *88*, 611-624.

Torres-Berrío, A., Lopez, J. P., Bagot, R. C., Nouel, D., Dal Bo, G., Cuesta, S., Zhu, L., Manitt, C., Eng, C., Cooper, H. M., Storch, K. F., Turecki, G., Nestler, E. J., and Flores, C. (2017). DCC Confers Susceptibility to Depression-like Behaviors in Humans and Mice and Is Regulated by miR-218. Biol Psychiatry *81*, 306-315.

Torres-Berrío, A., Morgunova, A., Giroux, M., Cuesta, S., Nestler, E. J., and Flores, C. (2020b). miR-218 in Adolescence Predicts and Mediates Vulnerability to Stress. Biol Psychiatry

Torres-Berrío, A., Nouel, D., Cuesta, S., Parise, E. M., Restrepo-Lozano, J. M., Larochelle, P., Nestler, E. J., and Flores, C. (2020c). MiR-218: a molecular switch and potential biomarker of susceptibility to stress. Mol Psychiatry *25*, 951-964.

Via, E., Fullana, M. A., Goldberg, X., Tinoco-González, D., Martínez-Zalacaín, I., Soriano-Mas, C., Davey, C. G., Menchón, J. M., Straube, B., Kircher, T., Pujol, J., Cardoner, N., and

Harrison, B. J. (2018). Ventromedial prefrontal cortex activity and pathological worry in generalised anxiety disorder. Br J Psychiatry *213*, 437-443.

Wallis, C. U., Cockcroft, G. J., Cardinal, R. N., Roberts, A. C., and Clarke, H. F. (2019). Hippocampal Interaction With Area 25, but not Area 32, Regulates Marmoset Approach-Avoidance Behavior. Cereb Cortex *29*, 4818-4830.

Way, B. M., Laćan, G., Fairbanks, L. A., and Melega, W. P. (2007). Architectonic distribution of the serotonin transporter within the orbitofrontal cortex of the vervet monkey. Neuroscience *148*, 937-948.

Yoshino, Y., and Dwivedi, Y. (2020). Non-Coding RNAs in Psychiatric Disorders and Suicidal Behavior. Front Psychiatry *11*, 543893.

Zeredo, J. L., Quah, S. K. L., Wallis, C. U., Alexander, L., Cockcroft, G. J., Santangelo, A. M., Xia, J., Shiba, Y., Dalley, J. W., Cardinal, R. N., Roberts, A. C., and Clarke, H. F. (2019). Glutamate Within the Marmoset Anterior Hippocampus Interacts with Area 25 to Regulate the Behavioral and Cardiovascular Correlates of High-Trait Anxiety. J Neurosci *39*, 3094-3107.

Zhang, Y., Du, L., Bai, Y., Han, B., He, C., Gong, L., Huang, R., Shen, L., Chao, J., Liu, P., Zhang, H., Zhang, H., Gu, L., Li, J., Hu, G., Xie, C., Zhang, Z., and Yao, H. (2020). CircDYM ameliorates depressive-like behavior by targeting miR-9 to regulate microglial activation via HSP90 ubiquitination. Mol Psychiatry *25*, 1175-1190.

STAR METHODS

Subjects

For this study 6 adult male common marmosets, Callithrix jacchus, (26 ± 2 mo, 413 ± 17 g) balanced for SLC6A4 genotype were used in this study (Supplementary table 1). All animals had MRI and [18F]altanserin PET scans, human intruder (HI) test, and snake testing (procedures described previously by (Shiba et al., 2014)) before entering a pharmacological study, which consisted of repeated HI test with acute intramuscular (i.m.) doses of citalopram (behavioral data reported elsewhere (Santangelo et al., 2016)) and, after 2 months, with the 5HT2A antagonist M100907 (Santangelo et al., 2019) . Marmosets were bred onsite at the Innes Marmoset Colony (Behavioral and Clinical Neuroscience Institute) and housed as male-female pairs (males were vasectomized). Temperature (24 °C) and humidity (55%) conditions were controlled, and a dawn/dusk-like 12-h period was maintained. They were provided with a balanced diet and water ad libitum. This research has been regulated under the Animals (Scientific Procedures) Act 1986 Amendment Regulations 2012 following ethical review by the University of Cambridge Animal Welfare and Ethical Review Body.

Behavioral testing

The human intruder test involves measuring the animal's behavioral response to an unfamiliar human, the "human intruder," who stands in front of the animal's home-cage and maintains eye contact with the animal. Since animals bred in the laboratory have prior positive and negative experiences with human encounters, e.g., receiving food treats or being restrained for husbandry or experimental purposes, the unfamiliar "human intruder" acts as a threat with low probabilistic imminence and creates an

anxiety-provoking context. Avoidance and vigilance during the task are similar to human anxious behavior and sensitive to anxiolytics (Carey et al., 1992).

The procedure for the human intruder test is based on the method used by (Santangelo et al., 2016). Cameras and microphones are routinely present in the room for recording purposes such that all animals are habituated to the presence of recording equipment. Before the testing session begins, a camera and microphone are set up in front of the animal's home-cage. The animal was tested in the top-right quadrant of their home cage. During testing, the cagemate was separated from the subject and restricted to the left half of the home cage and was obscured from both the human intruder and the subject. After 8 min of being separated, an experimenter (unfamiliar to the animal) wearing a realistic latex human mask (Greyland Film, UK) and standard lab attire stood 40 cm from the cage and maintained eye contact with the subject for 2 min (intruder phase). Recording continued for a further 5 min after the intruder left (recovery phase). Behavior and vocalizations during the intruder phase were scored.

The model snake test involves recording the animal's behavioral response to a rubber snake which acts as an inherent predatory stimulus, provoking an innate fear response (Barros et al., 2000). Furthermore, as the model snake is placed directly within the homecage, the model snake presents far higher spatial threat imminence compared to the intruder in the human intruder test (Mobbs et al., 2020).

The procedure of the model snake test is based on the methods in (Shiba et al., 2014). Before the testing session begins, wireless cameras and a microphone are placed to record the animal's behavior from a top-down view and a frontal view. During a test session, the animal is separated from their cagemate and restricted to the upper right quadrant of their home cage, while the cagemate was separated by opaque dividers

to the left half of the home cage and cannot see into the testing quadrant. The 20-min test session is divided into four 5-min phases: a separation phase, where only the camera and microphone were present; a pre-snake phase, where an empty box without the model snake (a 27 cm tall rubber model of a rearing cobra) is placed in the test quadrant; a snake phase, where the empty box from the previous phase is replaced with a box containing the model snake (a sliding door is removed to expose the model snake once the box is in position); and a post-snake phase, where the empty box from the pre-snake phase is re-introduced into the test quadrant. Analyzed behaviors are summarized in Supplementary Table 2.

Genotyping

Genomic DNA (gDNA) was extracted from hair follicles of the back of the animals using using the QIAamp DNA Micro kit for forensic casework samples (Qiagen) (yield 0.5–1.2 µg per sample). Primers were designed to flank the SLC6A4 repeat region (Supplementary Table 3). HotStarTaq Plus DNA Polymerase (Qiagen) was used in a BioRad C1000 thermal cycler (conditions: activa- tion 15min at 94°C; 44 cycles of 30s at 94°C, 30s at 55°C and 1 min at 72 °C; and termination 5 min at 72 °C). The PCR product was visualized in an agarose gel, purified using the Mini Elute PCR Purification Kit (Qiagen) and sent for sequencing (Source BioScience, Cambridge, UK). Primers used for sequencing can be found in Supplementary Table 3.

Sample preparation

At the end of the study, animals were premedicated with ketamine hydrochloride before being euthanized with pentobarbital sodium (Dolethal; 1 mL of a 200-mg/mL solution; Merial Animal Health). Brain were dissected, frozen using liquid nitrogen, and

then sliced in a cryostat at −20 °C to 200-µm-thick sections. Tissue samples for each target region were excised using punches of 1.0 and 1.5-mm radio length. Eight punches per target region were used in this study (4 from the right hemisphere and 4 from the left hemisphere).

Nuclei isolation and sorting

8 punches/area/animal were used. Nuclei extraction protocol was adapted from Halder et al. (2016). All steps were performed at 4 °C or on ice. Tissues were homogenized in nuclei isolation buffer (0.32 M Sucrose, 10 mM HEPES pH 8.0, 5 mM $CaCl_2$, 3 mM $Mg(CH_3COO)_2$, 0.1 mM EDTA, 1 mM DTT, 0.1% Triton X-100) with a 2 ml Dounce homogenizer by 10 gentle strokes with each pestle and filtered through a 40 µm strainer. After centrifugation, nuclei pellets were resuspended in 1 ml PBS-RI (PBS, 50 U/mL Rnase-OUT Recombinant Ribonuclease Inhibitor (Invitrogen), 1 mM DTT) and fixed by the addition of 3 ml PBS 1.33% paraformaldehyde (Electron Microscopy Sciences) for 30 minutes on ice. Fixed nuclei were spun down, washed with 1 ml PBS 0.1% triton-X-100, pelleted again and resuspended at 10^6 nuclei per ml in stain/wash buffer (PBS-RI, 0.5% BSA, 0.1% Triton-X-100) containing 2 µg/ml anti-NeuN-alexa-488 antibody (Millipore, MAB377X) and 1 µg/ml Hoechst 33342 (Molecular Probes). After 30 minutes incubation on ice protected from light, nuclei were washed with 2 mL stain/wash buffer and spun down. Finally, stained nuclei were resuspended in 1 ml PBS-RI 0.5% BSA and filtered again through a 40 µm strainer. Nuclei suspensions were maintained on ice protected from light until sorting.

Sorting of nuclei was achieved with a MoFlo Astrios EQ Cell sorter (Beckman Coulter). After positive selection of intact Hoechst-positive nuclei and doublets exclusion, all NeuN-positive and NeuN-negative nuclei were separately isolated. Sorted nuclei were

collected in refrigerated 2 ml microtubes containing 0.5 ml PBS-RI 0.5% BSA. Finally, nuclei were spun down, supernatants eliminated and pellets were conserved at -80°C untill RNA extraction.

RNA extraction and reverse transcription

Total RNAs (small and large RNAs) were extracted in one fraction with miRNeasy FFPE kit (Qiagen) following manufacturer's protocol with minor changes. Briefly, nuclei pellets were lysed in 150 µL PKD buffer and 10 µl proteinase K for 15 minutes at 56°C, then immediately incubated at 80°C for 15 minutes in order to reverse formaldehyde modification of nucleic acids and then immediately incubated 3 minutes on ice. After centrifugation, supernatants were transferred in new 2 ml microtubes and remaining DNA was degraded during a 30 minutes incubation with DNase Booster Buffer and DNase I. Addition of RBC buffer and ethanol allowed RNA binding to MiniElute spin columns. After washing steps, pure RNAs were eluted with 20 µl of RNase-free water. Total RNA concentrations were determined with a Nanodrop spectrophotometer (Fisher Scientific).

miRNA reverse transcription and quantification

miRNAs were specifically reverse transcribed with TaqMan Advanced miRNA cDNA Synthesis Kit (Applied Biosystems). Depending on RNA concentration, 10 ng or 2 µl total RNA were used as starting material for each poly(A) tailing reaction, followed by adaptor ligation and reverse transcription. We chose not to perform the last pre-amplification reaction in order to avoid eventual amplification bias.

The expression level of 752 miRNAs was screened by real-time PCR with TaqMan Advanced miRNA Human A and B Cards (Applied Biosystems A31805). cDNAs were

diluted 1:10 with 0.1X TE buffer, then mixed with water and TaqMan Fast Advanced Master Mix 2X (Applied Biosystems) and 100 µL of this mix was loaded in each fill reservoir of two array cards. Real-time PCR reactions were run on a QuantStudio 7 Flex Real-Time PCR System (Applied Biosystems).

mRNA reverse transcription and quantification

40 ng total RNAs were reverse transcribed with SuperScript IV Reverse Transcriptase (Invitrogen) and random hexamers in 30 µl total reaction volumes. cDNAs were diluted with water and 266 pg of cDNA was used in each 20 µl-PCR reaction in 96-well plates. Gene expression was quantified by real-time PCR with marmoset specific TaqMan Gene Expression Assays (Applied Biostems) and TaqMan Fast Advanced Master Mix (Applied Biosystems) on a QuantStudio 7 Flex Real-Time PCR System (Applied Biosystems).

Data analysis

Data were revised and analyzed using ThermoFisher Scientific Digital Science online tools (thermofisher.com/fr/en/home/digital-science.html). Relative quantification was performed with the $\Delta\Delta$Ct method.

368 miRNAs were robustly amplified and were considered for subsequent analysis. DeltaCt values were obtained by global normalization method. qPCR results were first normalized (using global mean normalization method) and then transformed to relative expression levels via the $2^{-\Delta Ct}$ equation.

Four references genes were used as endogenous control genes (POLR2A, TBP, HPRT1, PGK1). DeltaCt values were obtained by subtracting the mean Ct value of these 4 control genes to the Ct value of each target gene.

For behavioral experiments, EFA in HI test or snake model tests were extracted as previously described (Quah et al., 2020b).

Statistics

All values were represented as scatterplot with the mean ± SEM. Statistical analysis was performed using XLStat (PCA), GraphPad 7.0 (ANOVA, correlation analysis and t-tests) and R (PCA and regression analysis). A significance threshold of a 0,05 was used in all experiments.

Statistical differences between two groups were analyzed with Student's t tests. Correlations were calculated using the Pearson correlation coefficient with 2-tailed analysis. Otherwise, 1- or 2-way analyses of variance were performed. No statistical methods were used to determine the sample sizes, but the number of experimental subjects is similar to sample sizes routinely used in our laboratory and in the field for similar experiments. All data were normally distributed and variance was similar between groups, supporting the use of parametric statistics. Statistical differences were set to $p<0.05$.

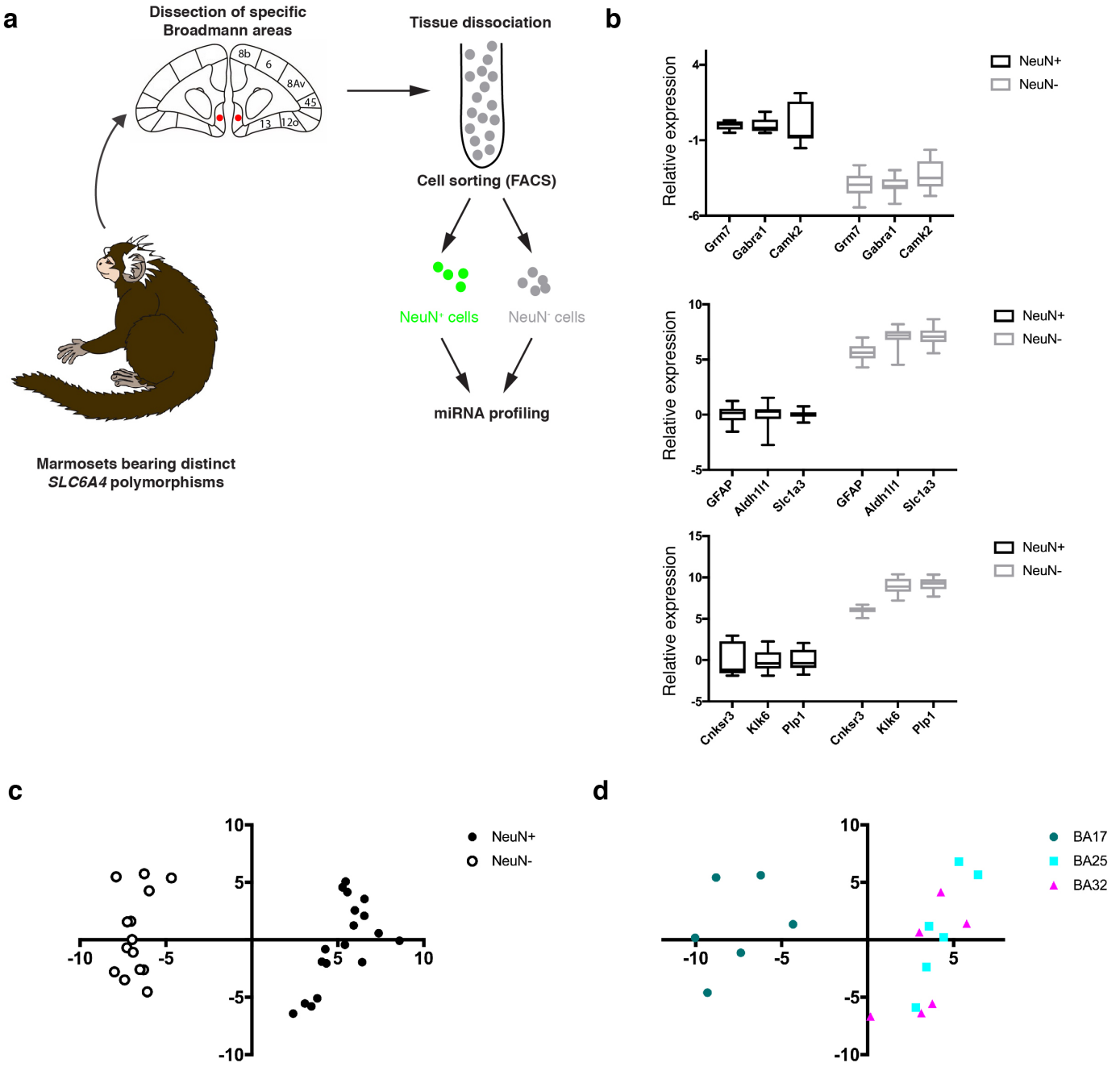

Figure 1. Schematic representation of experimental protocol and validation steps.
a) Experimental protocol include the genotypic and phenotypic characterization of the marmosets. After sacrifice, brains were frozen and sliced without fixation. RNA was extracted from punches of different cortical regions. Samples were previously submitted to nuclear isolation, NeuN staining and FACS sorting.
b) Expression of neuronal (top panel), astrocytic (middle panel) and oligodendrocytic (bottom panels) markers in NeuN$^+$ and NeuN$^-$ fractions confirms the efficiency of the FACS sorting strategy.
c) PCA analysis on the levels of 92 miRNAs expressed in both NeuN$^+$ and NeuN$^-$ nuclei demonstrate that miRNAs profiles clearly differentiate both fractions.
d) PCA analysis on miRNAs level in NeuN$^+$ fraction enables regional discrimination. Samples from the visual clearly cluster apart from those of the vmPFC which, in turn, are intermingled.

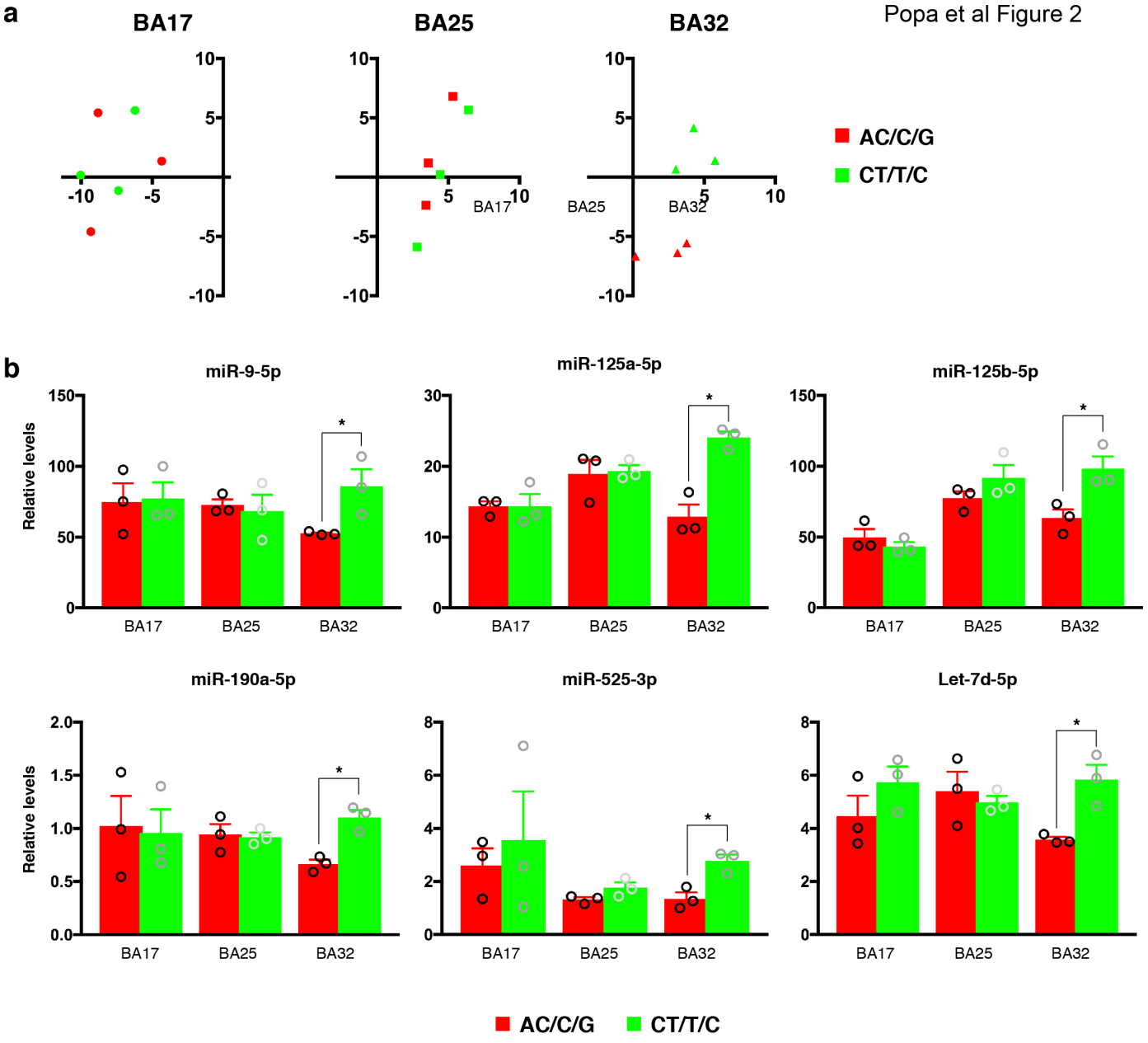

Figure 2. Slc6a4 polymorphisms (AC/C/G and CT/T/C) alter miRNA signature in area 32.
a) PCA analysis on miRNAs level in NeuN⁺ nuclei shows genotypic differences only in area 32.
b) Top miRNAs differentially expressed in area 32 in AC/C/G and CT/T/C marmosets (One way ANOVA fo llowed by Bonferroni's test for multiple comparisons, * p<0.05).

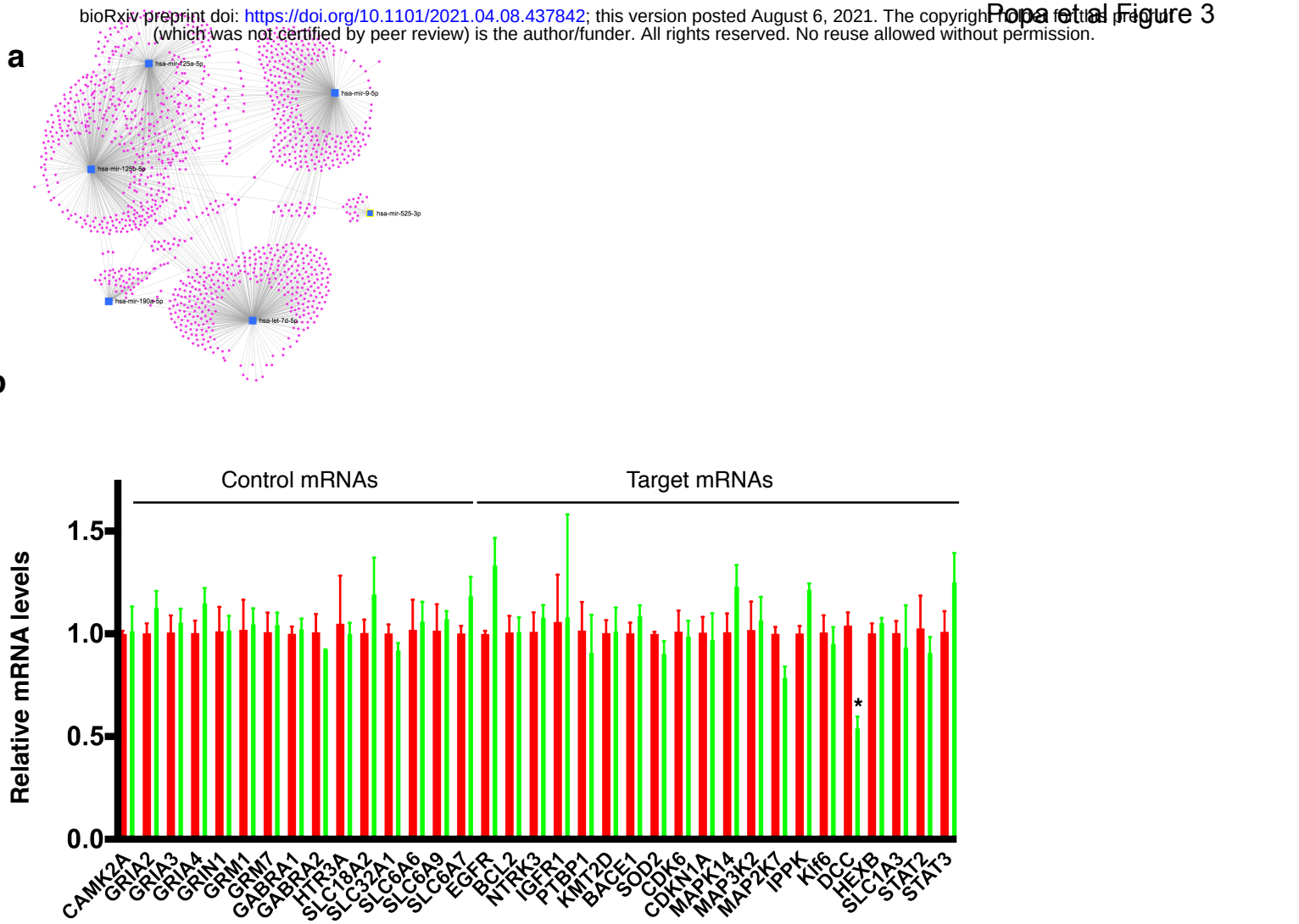

Figure 3. Target mRNAs in area 32.
a) Network analysis using miRNAs deregulated in area 32.
b) Expression of target mRNAs identified by network analysis in area 32. Using as reference the AC/C/G geno type, we measured the abundance of 20 potential targets as well as 15 reference genes. Only DCCwas found to be differentially expressed in area 32 (* $p<0.05$, t-test)

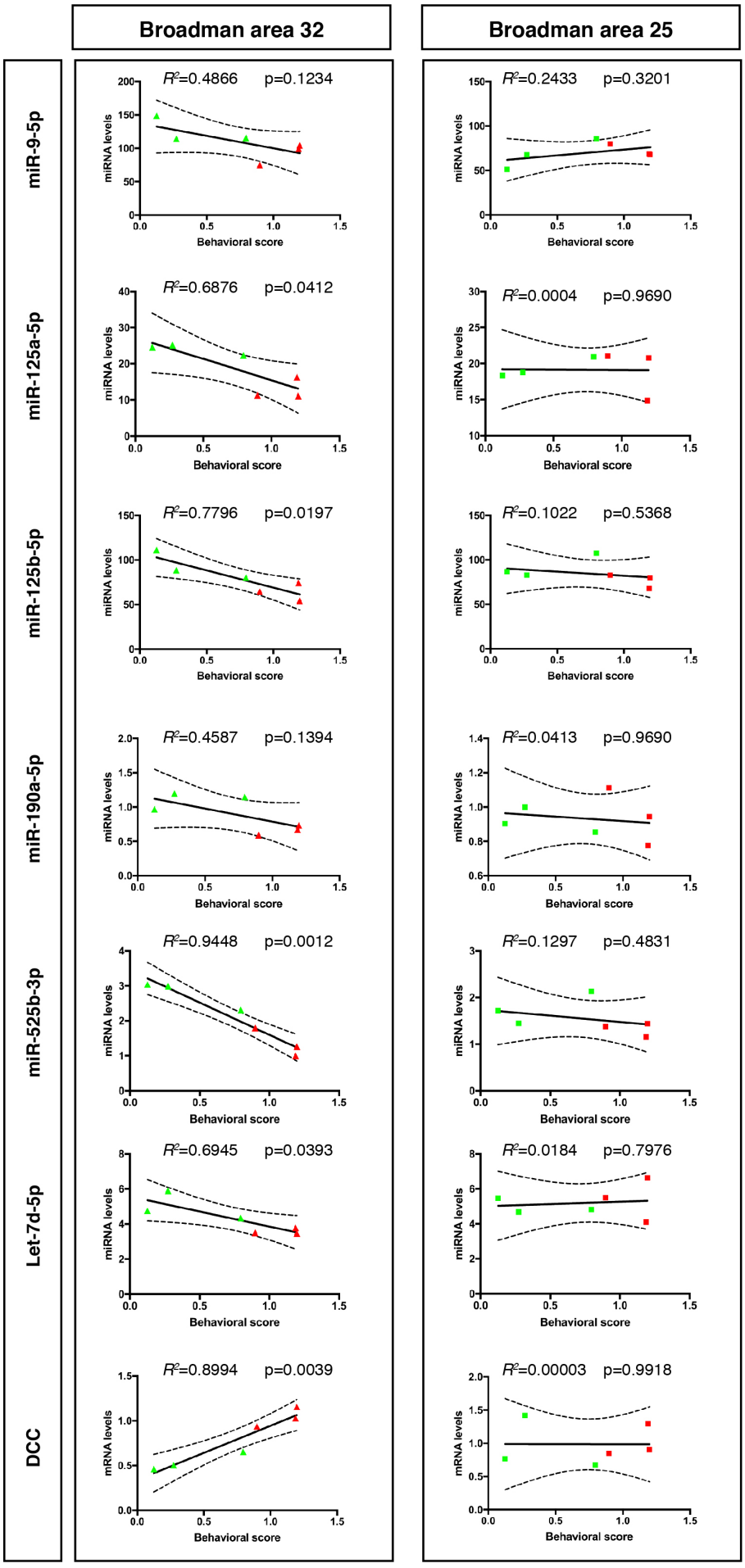

Figure 4. Correlation between miRNA and Dcc levels in area 32 (leftpanels) or 25 (right panels) and behavioral response in the human intruder test.